Astrophysics and Space Science manuscript No.
(will be inserted by the editor)

Frank Haberl

The Magnificent Seven: Magnetic fields and surface temperature distributions

arXiv:astro-ph/0609066v1 4 Sep 2006

Received: date / Accepted: date

Abstract Presently seven nearby radio-quiet isolated neutron stars discovered in ROSAT data and characterized by thermal X-ray spectra are known. They exhibit very similar properties and despite intensive searches their number remained constant since 2001 which led to their name "The Magnificent Seven". Five of the stars exhibit pulsations in their X-ray flux with periods in the range of 3.4 s to 11.4 s. XMM-Newton observations revealed broad absorption lines in the X-ray spectra which are interpreted as cyclotron resonance absorption lines by protons or heavy ions and / or atomic transitions shifted to X-ray energies by strong magnetic fields of the order of 10^{13} G. New XMM-Newton observations indicate more complex X-ray spectra with multiple absorption lines. Pulse-phase spectroscopy of the best studied pulsars RX J0720.4–3125 and RBS 1223 reveals variations in derived emission temperature and absorption line depth with pulse phase. Moreover, RX J0720.4–3125 shows long-term spectral changes which are interpreted as due to free precession of the neutron star. Modeling of the pulse profiles of RX J0720.4–3125 and RBS 1223 provides information about the surface temperature distribution of the neutron stars indicating hot polar caps which have different temperatures, different sizes and are probably not located in antipodal positions.

Keywords stars: neutron · stars: magnetic fields · X-rays: stars

PACS

1 Introduction

After the discovery of RX J1856.4–3754 as an isolated neutron star in ROSAT data (Walter et al. 1996; Walter & Matthews 1997), six further objects with very similar properties were found. Their X-ray emission is characterized by a soft, blackbody-like continuum which is little attenuated by photo-electric absorption by the interstellar medium, indicating small distances (of the order of a few 100 pc, Posselt et al. 2006). For the brightest object, RX J1856.4–3754, this was soon confirmed by the parallax measurement (Walter 2001; Kaplan et al. 2002c; Walter & Lattimer 2002). Including new HST observations the most recent revision of the parallax yields a distance of 161^{+18}_{-14} pc (van Kerkwijk & Kaplan 2006). A preliminary value for the parallax of RX J0720.4–3125 is presented by van Kerkwijk & Kaplan (2006) which corresponds to a distance of 330^{+170}_{-80} pc.

No indication for a hard, non-thermal X-ray emission component was found in the X-ray spectra. Compared to normal radio pulsars also no strong radio emission is detected: While for RX J0720.4–3125 and RX J0806.4–4123 deep radio observations failed to detect a radio counterpart (Johnston 2003; Kaplan et al. 2003b), for RBS 1223 and RBS 1774 the detection of weak radio emission was claimed (Malofeev et al. 2006b,a). The constant X-ray flux on time scales of years, no obvious association with a supernova remnant and relatively high proper motion measurements for the three brightest objects suggest that we deal with a group of cooling neutron stars with ages of around 10^6 years. Recent reviews which summarize the observed properties of the seven thermally emitting INSs known today can be found in Treves et al. (2000), Motch (2001) and Haberl (2004, 2005).

The discovery of the seven neutron stars (which are often called the Magnificent Seven, hereafter M7) with purely thermal X-ray spectra raised wide interest by theoreticians and observers as promising objects to learn about atmospheres and the internal structure of neutron stars (e.g. Paerels 1997). The apparent absence of non-thermal processes which would hamper the analysis of the X-ray emission allows a direct view onto the stellar surface. Limits on the radius of the star RX J1856.4–3754 were used to constrain the equation of state of neutron star matter (Pons et al. 2002; Trümper et al.

F. Haberl
Max-Planck-Institut für extraterrestrische Physik
Giessenbachstrasse, 85748 Garching, Germany
Tel.: +49-89-300003320
Fax: +49-89-300003569
E-mail: fwh@mpe.mpg.de

Table 1 X-ray and optical properties of the Magnificent Seven

Object	kT eV	Period s	Amplitude %	Optical mag	PM mas/year	Ref.
RX J0420.0–5022	44	3.45	13	B = 26.6		1
RX J0720.4–3125	85-95	8.39	8-15	B = 26.6	97	2,3,4,5,6
RX J0806.4–4123	96	11.37	6	B > 24		7,1
RBS 1223$^{(a)}$	86	10.31	18	$m_{50ccd} = 28.6$		8,9,10,11
RX J1605.3+3249	96	6.88?	?	B = 27.2	145	12,13,14,15
RX J1856.5–3754	62	–	<1.3	B = 25.2	332	16,17,18,19
RBS 1774$^{(b)}$	102	9.44	4	B > 26		20,21,22

$^{(a)}$ = 1RXS J130848.6+212708
$^{(b)}$ = 1RXS J214303.7+065419
References:
(1) Haberl et al. (2004a) (2) Haberl et al. (1997) (3) Cropper et al. (2001)
(4) Haberl et al. (2004b) (5) de Vries et al. (2004) (6) Motch et al. (2003)
(7) Haberl & Zavlin (2002) (8) Schwope et al. (1999) (9) Hambaryan et al. (2002)
(10) Kaplan et al. (2002a) (11) Haberl et al. (2003) (12) Motch et al. (1999)
(13) Kaplan et al. (2003a) (14) van Kerkwijk et al. (2004) (15) Motch et al. (2005)
(16) Walter & Matthews (1997) (17) Walter & Lattimer (2002) (18) Burwitz et al. (2003)
(19) van Kerkwijk & Kulkarni (2001b) (20) Zampieri et al. (2001) (21) Zane et al. (2005) (22) Komarova (2006)

2004). The ROSAT PSPC spectra with low energy resolution were consistent with Planckian energy distributions with blackbody temperatures kT in the range 40 – 100 eV and little attenuation by interstellar absorption. More recent high resolution observations of the two brightest objects RX J1856.4–3754 (Burwitz et al. 2001) and RX J0720.4–3125 (Paerels et al. 2001; Pavlov et al. 2002; Kaplan et al. 2003b) were performed using the low energy transmission grating (LETG) aboard Chandra and the reflection grating spectrometers (RGS) of XMM-Newton. In particular the high signal to noise LETG spectrum from a 500 ks Chandra observation of RX J1856.4–3754 did not reveal any significant deviation from a blackbody spectrum (Burwitz et al. 2001, 2003). The statistical quality and energy band coverage of the RGS and LETG spectra of RX J0720.4–3125 are however insufficient to detect subtle narrow features in the spectrum (Paerels et al. 2001).

Four of the M7 exhibit clear pulsations in their X-ray flux, indicating the spin period of the neutron star (RX J0420.0–5022, RX J0720.4–3125, RX J0806.4–4123 and RBS 1223) and there is evidence that also RBS 1774 is a pulsar (Zane et al. 2005). A possible candidate period for RX J1605.3+3249 needs future confirmation. A summary with blackbody temperatures derived from (phase-averaged) EPIC-pn spectra, spin periods, amplitudes for the flux modulation, optical brightness and measured proper motions is given in Table 1 together with key references for each object. Despite extensive searches in ROSAT data (e.g. Rutledge et al. 2003; Chieregato et al. 2005; Agüeros et al. 2006) no further neutron star with similar characteristic properties was found.

The first significant deviations from a blackbody spectrum were reported by Haberl et al. (2003) from EPIC spectra of RBS 1223. A broad absorption feature near 300 eV was interpreted as proton cyclotron resonance absorption. Apart from this absorption line with an equivalent width of 160 eV the X-ray spectrum of RBS 1223 is blackbody-like. Haberl et al. (2003) also suggested that changes in the soft part of the X-ray spectrum of the pulsar RX J0720.4–3125 with pulse phase reported by Cropper et al. (2001) are caused by variable cyclotron absorption (Haberl et al. 2004b). Cyclotron resonance absorption features in the 0.1–1.0 keV band are expected in spectra from strongly magnetized neutron stars with field strengths in the range of $10^{10} - 10^{11}$ G or $2 \times 10^{13} - 2 \times 10^{14}$ G if caused by electrons or protons, respectively (see e.g. Zane et al. 2001; Zavlin & Pavlov 2002). Variation of the magnetic field strength over the neutron star surface leads to a broadening of the line (Ho & Lai 2004).

The relatively long spin periods in the range of 3.45 s – 11.37 s (the majority of radio pulsars has periods less than 1 s) were the first indicator for strong magnetic fields. If the stars were born with millisecond spin periods, age estimates from neutron star cooling curves (Page et al. 2006) and proper motions (tracing the neutron star back to a likely birth place, Motch et al. 2006) of typically 10^6 years require B fields of the order of 10^{13} G to decelerate the rotation of the stars to their current periods. This was recently confirmed by the accurate determination of the pulse period derivative $\dot{P}$ of 0.698×10^{-13} s s^{-1} and 1.120×10^{-13} s s^{-1} for RX J0720.4–3125 and RBS 1223, respectively (Kaplan & van Kerkwijk 2005a,b). In the magnetic dipole braking model this yields characteristic ages of 1.9×10^6 years and 1.5×10^6 years and B field strengths of 2.4×10^{13} G and 3.4×10^{13} G, respectively. Such strong fields supports the picture in which the broad absorption lines – if due to cyclotron resonance – at least for RX J0720.4–3125 and RBS 1223 are caused by protons.

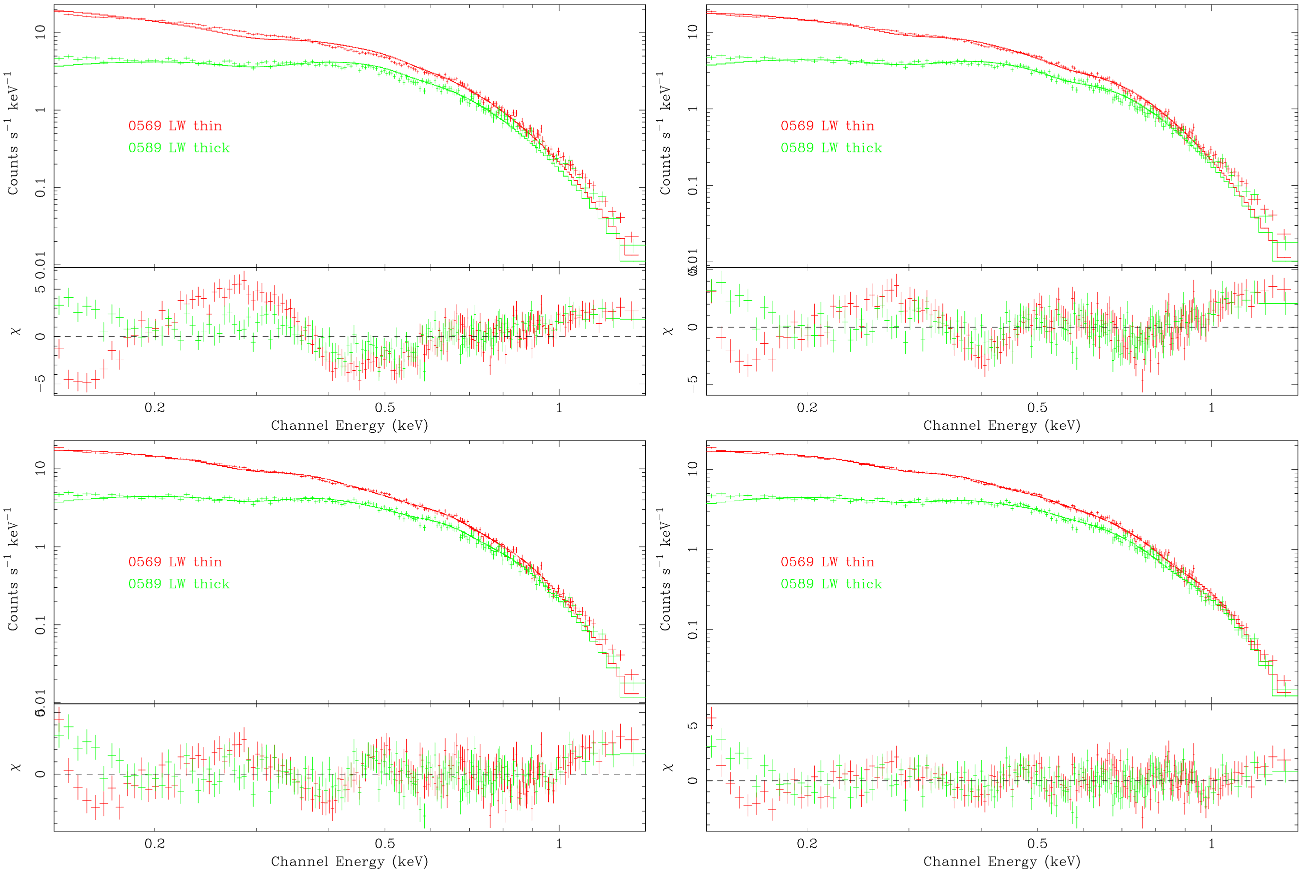

Fig. 1 Modeling of the EPIC-pn spectra of RX J1605.3+3249. From top left to bottom right the number of absorption lines increases from zero to three. As continuum a blackbody model with interstellar absorption is used.

2 Pulse-phase averaged X-ray spectra

Significant deviations from the absorbed blackbody spectrum were reported from XMM-Newton EPIC observations of RBS 1223 (Haberl et al. 2003) and RX J0720.4–3125 (Haberl et al. 2004b) and from XMM-Newton RGS spectra of RX J1605.3+3249 (van Kerkwijk et al. 2004). Also non-magnetic neutron star atmosphere models (e.g. Gänsicke et al. 2002; Zavlin & Pavlov 2002) fail to reproduce the spectra. Iron and solar mixture atmospheres cause too many absorption features in particular at energies between 0.5 and 1.0 keV which are not seen in the measured spectra. On the other hand the spectrum of a pure hydrogen model is similar in shape to that of a blackbody but results in a much lower effective temperature which would predict a far too high optical flux (see Pavlov et al. 1996). The modeling of the X-ray spectra was significantly improved by including a broad absorption line with Gaussian shape. Line energies around 300 eV were found for RX J0720.4–3125 and RBS 1223 from the medium energy resolution EPIC spectra, while a line with higher energy of 450 – 480 eV was discovered in the high energy resolution RGS spectrum of RX J1605.3+3249.

Spectral fits to the EPIC-pn spectra of the third brightest M7 star RX J1605.3+3249 obtained in 2003, January 17 and February 26 (satellite revolutions 569 and 589) also considerably improve when adding a Gaussian absorption line to the absorbed blackbody model (see Table 2 and Fig. 1). However, the quality of the fit with a reduced χ^2 of 2.39 (all XMM-Newton spectra presented here were obtained using the analysis software SAS version 6.5) is still not acceptable and worse than typical values around 1.5 one finds for joint fits to the available EPIC-pn spectra of RX J1856.4–3754 (see Fig. 2) or RX J0720.4–3125. Adding more lines further improves the fit quality and with three absorption lines an acceptable χ^2 is found. The best fit parameters for the models with different number of absorption lines are listed in Table 2. The width of the lines was fit as a single common parameter in the case of multiple lines (σ = 87 eV for the model with three lines). A remarkable result is the ratio of the line energies for the model with three lines. With E_2/E_1 = 1.46±0.02 and E_3/E_1 = 1.94±0.06 the line energy ratios are consistent with 1:1.5:2. It should also be noted that the depth of the lines decreases with line energy by a factor of about 5 (in terms of absorbed line photon flux) from one line to

Table 2 Model fits to the EPIC-pn spectra of RX J1605.3+3249

N_H 10^{20} cm^{-2}	kT eV	E_1 eV	E_2 eV	E_3 eV	F_1	F_2 10^{-4} photons cm^{-2} s^{-1}	F_3	EW_1 eV	EW_2 eV	EW_3 eV	χ^2_{red}
0.15	97	–	–	–	–	–	–				4.38
1.1	92	445	–	–	−67	–	–				2.39
1.4	92	440	1.5E_1	–	−75	−43	–				1.75
2.04±0.04	91.6±0.3	403±2	589±4	780±24	−43±1	−8.0±0.8	−1.6±0.4	96	76	67	1.39

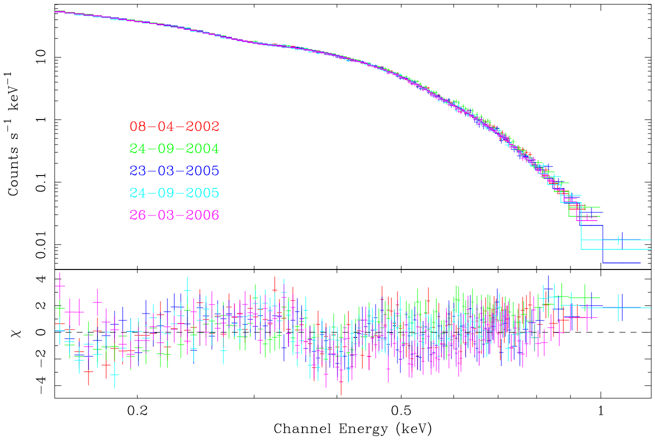

Fig. 2 EPIC-pn spectra of RX J1856.4–3754 obtained from five observations between 2002 and 2006 with the same instrumental setup (small window readout mode and thin filter). A joint fit with an absorbed blackbody model yields a reduced χ^2 of 1.55 and demonstrates the stability of detector and source to better than 1%. The dip in the residuals around 0.4 keV is a remaining calibration problem.

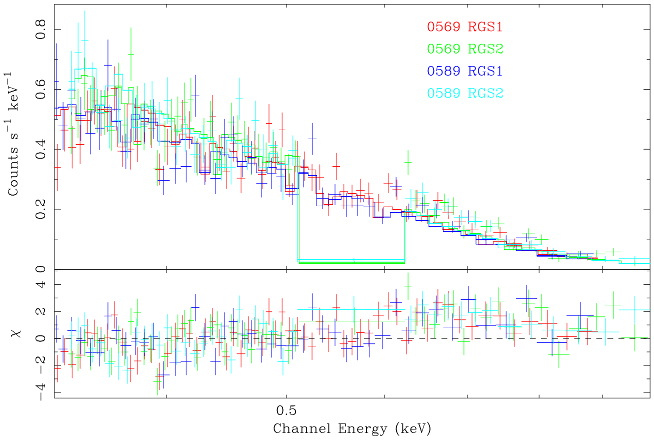

Fig. 3 RGS spectra of RX J1605.3+3249 from the two observations in 2003, January 17 and February 26 (satellite revolutions 569 and 589). The histograms represent the best fit EPIC-pn model with three absorption lines allowing only a re-normalization to account for possible cross-calibration problems.

the next. A fit with the model with three absorption lines to the RGS spectra (only allowing a re-normalization factor between the instruments) shows that also the RGS spectra are consistent with that model (Fig. 3).

Similar to RX J1605.3+3249, new XMM-Newton observations also indicate a more complex X-ray spectrum for RBS 1223. With a total exposure time of more than 100 ks the increased statistical quality of the EPIC-pn spectra requires two absorption lines for an acceptable fit (Schwope et al. 2006). With 230 eV and 460 eV the line energies are a factor of two apart. Also, in the case of RX J0806.4–4123 a simple absorbed blackbody model yields an unacceptable fit to the EPIC-pn spectra (Haberl et al. 2004a). A model with one line results in χ^2_{red} = 1.39 which is formally acceptable. Adding another line with an energy twice that of the first one, further improves the fit to χ^2_{red} = 1.05, but more higher quality data is required to confirm the significance of this result.

Table 3 summarizes the magnetic field estimates for the M7 neutron stars utilizing either the magnetic dipole braking model for the pulsars with measured pulse period derivative $\dot{P}$ ($B = 3.2 \times 10^{19} (P \times \dot{P})^{1/2}$) or assuming that the absorption line is due to cyclotron resonance by protons ($B = 1.6 \times 10^{11} E(eV)/(1 - 2GM/c^2R)^{1/2}$). If multiple absorption lines were included in the spectral modeling, the lowest line energy was used for the estimate of the magnetic field.

The brightest M7 star, RX J1856.4–3754, does not show pulsations with a very low amplitude limit of 1.3% (Ransom et al. 2002; Burwitz et al. 2003). However, van Kerkwijk & Kull (2001a) discovered the existence of a Hα nebula around the star with cometary-like morphology aligned with the direction of its proper motion. Assuming that the nebula is powered by magnetic dipole braking and an age of the neutron star of ∼5 $\times 10^5$ years which is inferred from its proper motion and the distance to the likely birth place, a magnetic field strength of ∼1 × 10^{13} G is derived (Kaplan et al. 2002c; Braje & Romani 2002; Trümper et al. 2004). Such a field strength is consistent with the non-detection of a proton cyclotron feature which would have an energy below the sensitive range of X-ray instruments.

In two cases (RX J0720.4–3125 and RBS 1223) accurate $\dot{P}$ measurements exist. For both stars also absorption lines were found in their X-ray spectra which allows a comparison of B_{db} (field estimate from dipole braking) and B_{cyc} (field estimate from proton cyclotron resonance). The ratio B_{cyc}/B_{db} is 2.33 for RX J0720.4–3125 and 1.35 for RBS 1223 (for the spectral model with two lines). A similar low ratio for RX J0720.4–3125 would be

Table 3 Magnetic field estimates

Object	dP/dt 10^{-13} ss^{-1}	E_{cyc} eV	B_{db} 10^{13} G	B_{cyc} 10^{13} G
RX J0420.0−5022	<92	330	<18	6.6
RX J0720.4−3125	0.698(2)	280	2.4	5.6
RX J0806.4−4123	<18	430/306$^{(a)}$	<14	8.6/6.1
RBS 1223	1.120(3)	300/230$^{(a)}$	3.4	6.0/4.6
RX J1605.3+3249		450/400$^{(b)}$		9/8
RX J1856.5−3754		–	∼1$^{(c)}$	
RBS 1774	<60$^{(d)}$	750	<24$^{(d)}$	15

$^{(a)}$ Spectral fit with single / two lines
$^{(b)}$ With single line / three lines at 400 eV, 600 eV and 800 eV
$^{(c)}$ Estimate from Hα nebula assuming that it is powered by magnetic dipole breaking (Kaplan et al. 2002c; Braje & Romani 2002; Trümper et al. 2004)
$^{(d)}$ Radio detection: Malofeev et al. (2006b)

obtained if a second (lower-energy) line around 140 eV exists. Unfortunately, the detection of a line at such low energies is outside the capability of the XMM-Newton instruments.

3 Neutron star surface temperature distributions

The first XMM-Newton observations of RX J0720.4–3125 revealed spectral changes with pulse phase expressed as hardness ratio variations (Cropper et al. 2001). Using polar cap models first constraints on the polar cap sizes and viewing geometries could be derived. The pulse profile in the 0.12 keV to 1.2 keV energy band was found to be approximately sinusoidal with a peak-to-peak amplitude of about 15% with the hardness ratio being softest slightly before flux maximum. Spectra from different pulse phases indicated a temperature variation and a change in the low-energy attenuation, which - when modeled with a simple absorbed blackbody spectrum - appears as variable absorption column density. Including more data Haberl et al. (2004b) interpreted this as broad absorption line with variable depth. Pulse phase spectroscopy of RBS 1223 (Schwope et al. 2005) also revealed that changes in temperature and absorption line depth are responsible for the spectral variations with pulse phase. The double-humped X-ray light curves of RBS 1223 in different energy bands were modeled by Schwope et al. (2005) assuming Planckian radiation from a neutron star surface with inhomogeneous temperature distribution. Again, a simple model with two hot spots with temperatures $T_1^\infty = 92$ eV and $T_2^\infty = 84$ eV and full angular sizes of 8° and 10° which are separated by ∼ 160° can reproduce the data. A more physical temperature distribution based on the crustal field models by Geppert et al. (2004) which can produce relatively strong temperature gradients from the magnetic poles to the equator was equally successful.

The neutron star RX J0720.4–3125 is unique among the M7 as it shows a gradual change of its X-ray spectrum over years which is accompanied by an energy-dependent change in the pulse profile (de Vries et al. 2004; Vink et al. 2004). Figure 4 shows folded light curves together with hardness ratios for six different epochs. They were derived from observations with identical instrumental setup to avoid systematic differences between different filters and CCD readout modes. As was found by de Vries et al. (2004) the pulse profile became deeper with time with a pulsed fraction of ∼8% in the year 2000, increasing to ∼15% by the end of 2003. Moreover, the spectra became considerable harder during these years as can be seen in the increase of the average hardness ratio in Fig. 4. Haberl et al. (2006) found first evidence for a trend reversal of the spectral evolution and interpret the involved period of 7.1±0.5 years as precession period of the neutron star.

The overall hardening of the spectra until 2004 and the trend-reversal can also be seen from the pulse-phase resolved spectra which are shown in Fig. 5 for four different XMM-Newton observations. Both, pulse-phase variations and long-term spectral changes can be modeled by variations in the blackbody temperature and absorption line depth (Haberl et al. 2006). In Fig. 6 the line equivalent width is plotted versus temperature kT. The temperature variation (∼2.5 eV) was smaller during the first observations and increased to ∼6 eV, almost as large as the long-term change of ∼8 eV seen in the phase-averaged spectra. This supports the idea that the temperature changes are caused by geometrical effects and different areas on the neutron star surface come into our view. In contrast, the amplitude in the equivalent width variation is ∼40 eV and did not change much over the years. The relatively large variation in the line depth with pulse phase and the strong increase over the years indicates that the hotter polar cap which came into (better) view – possibly due to precession – plays the major role in the line absorption. More detailed analyses are

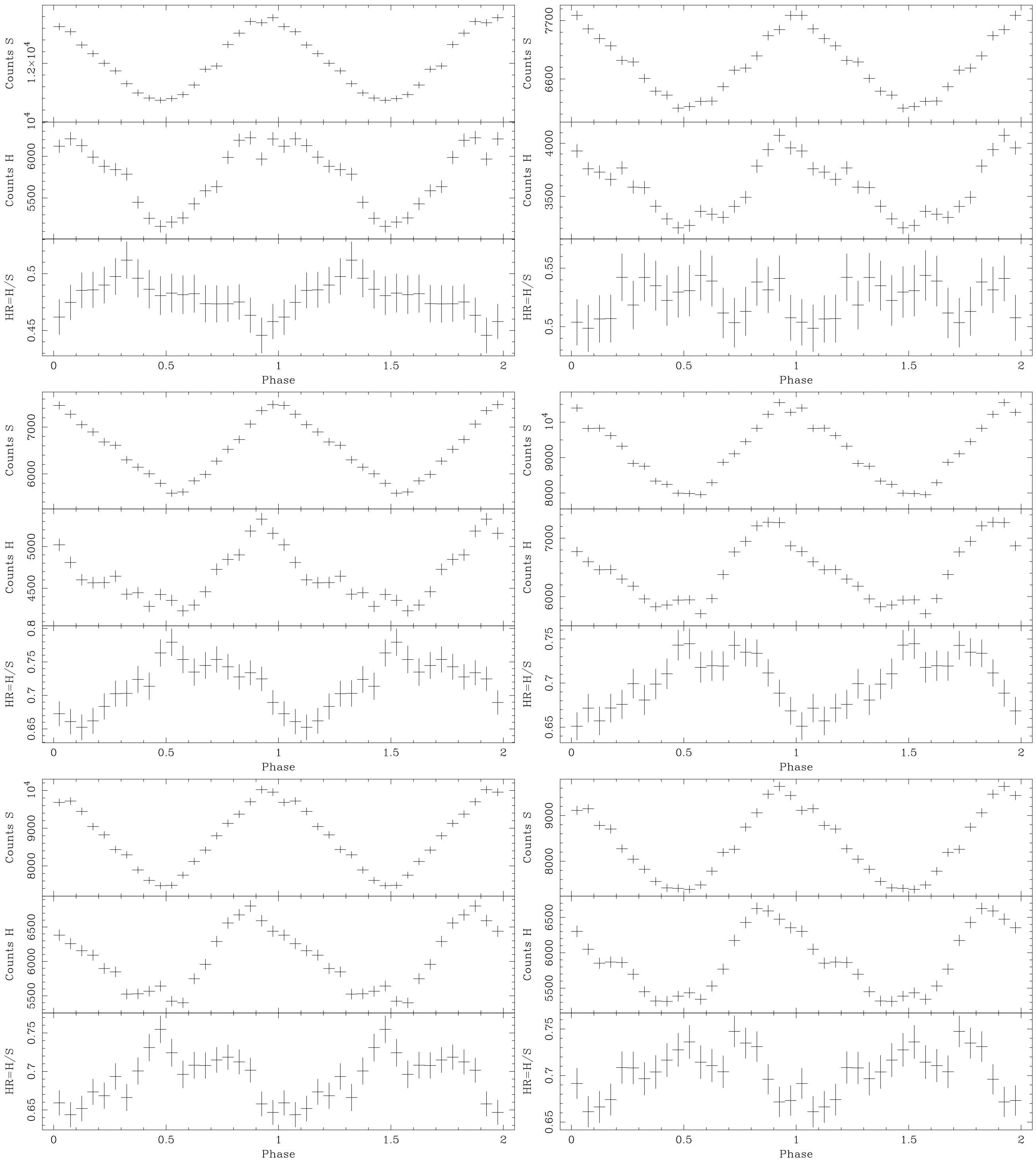

Fig. 4 Folded EPIC-pn light curves of RX J0720.4–3125 in two different energy bands (soft S: 120 eV - 400 eV; hard H: 400 eV - 1 keV) together with the hardness ratio. Different observations, all performed with the same instrumental setup (full-frame mode with thin filter), are shown from top left to bottom right: 2000 May 13, 2002 Nov. 6, 2004 May 22, 2005 April 28, 2005 Sep. 23 and 2005 Nov. 12. For a detailed summary of all XMM-Newton observation in the years 2000 to 2005 see Table 1 in Haberl et al. (2006). Pulse phases were calculated using the X-ray timing ephemerides ("All Data" solution) from Kaplan & van Kerkwijk (2005a).

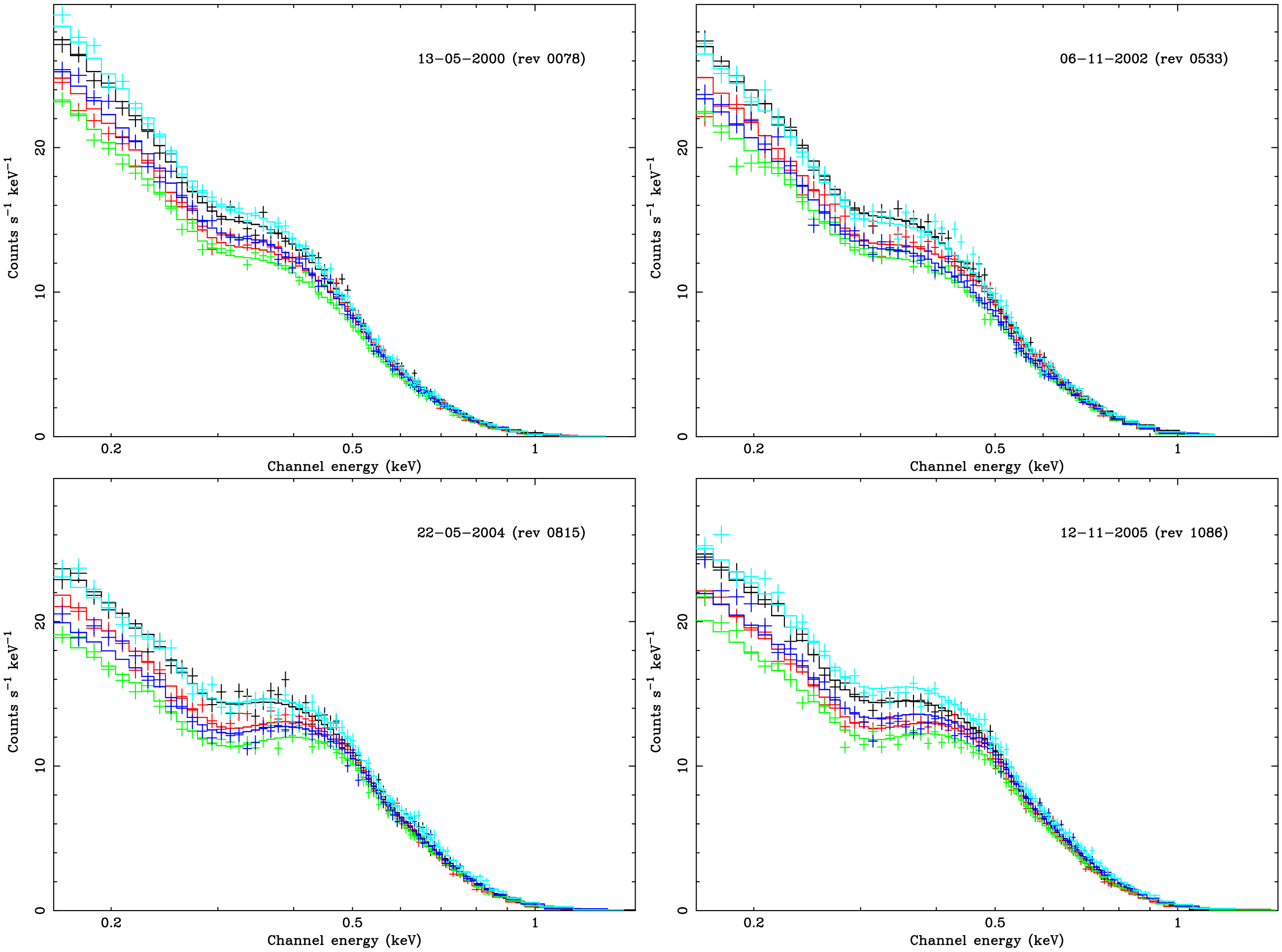

Fig. 5 Pulse-phase resolved EPIC-pn spectra of RX J0720.4–3125 from four different observations. During the pulse the spectra vary as is shown by the different colours used for different phases (0.0-0.2: black, 0.2-0.4: red, 0.4-0.6: green, 0.6-0.8: blue, 0.8-1.0: light blue; with phase 0.0 defined as intensity maximum as in Fig. 4). The intensity scale is linear to better resolve the changes at low energies.

required to see if this is mainly a temperature effect (for higher temperatures atomic line transitions are expected to be reduced because of a higher ionization degree) or a viewing effect due to the dependence on the angle between the direction of radiation propagation and magnetic field lines.

Since the spectral observations do not yet cover a complete precession period Haberl et al. (2006) also performed a preliminary analysis of published and new pulse timing residuals (from three new XMM-Newton observations). This includes archival ROSAT, Chandra and XMM-Newton observations which are distributed over a total of ~12 years (see Kaplan et al. 2002b; Zane et al. 2002; Cropper et al. 2004; Kaplan & van Kerkwijk 2005a). A sinusoidal fit to the phase residuals yields a period of 7.7±0.6 years (Fig. 7) consistent with that derived from the spectral analysis. In a similar analysis van Kerkwijk & Kaplan (2006) infer a shorter period of 4.3 years. Apart from using new Chandra data instead of the new XMM-observations they also used different phase residuals for the early ROSAT observations (which are subject to cycle count ambiguity) compared to the original values published in Kaplan & van Kerkwijk (2005a). The reason for the different periods might be due to the energy dependence of the pulse profile which can lead to systematic differences between instruments with different spectral response and/or the deviations from a sinusoidal shape of the light curves (which moreover evolve with time) as it was assumed in the analysis of Kaplan & van Kerkwijk (2005a). Further monitoring of RX J0720.4–3125 and a more sophisticated analysis and modeling of the data are required to confirm the precession model and further constrain its parameters. This can provide independent information about the interior of the neutron star and its distortion from a spherical shape $\epsilon = (I_3 - I_1)/I_1 = P_{spin}/P_{prec} \approx 4 \times 10^{-8}$ which is larger than that reported for radio pulsars (e.g. Jones & Andersson 2001; Akgün et al. 2006) but smaller than that for Her X-1 (Trümper et al. 1986; Ketsaris et al. 2000).

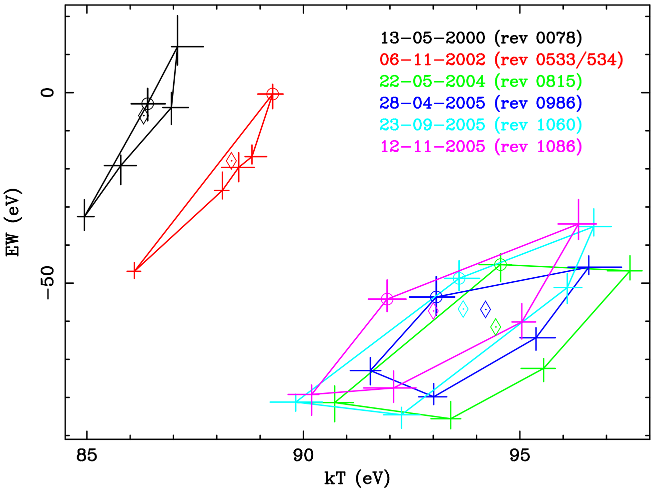

Fig. 6 Equivalent width of the absorption line vs. temperature kT derived from the EPIC-pn full-frame mode observations with thin filter. Diamonds denote the values derived from the phase-averaged spectra. During the pulse the parameters evolve counter-clockwise, the circle marks phase 0.0-0.2. This figure is a colour representation of Fig. 4 in Haberl et al. (2006).

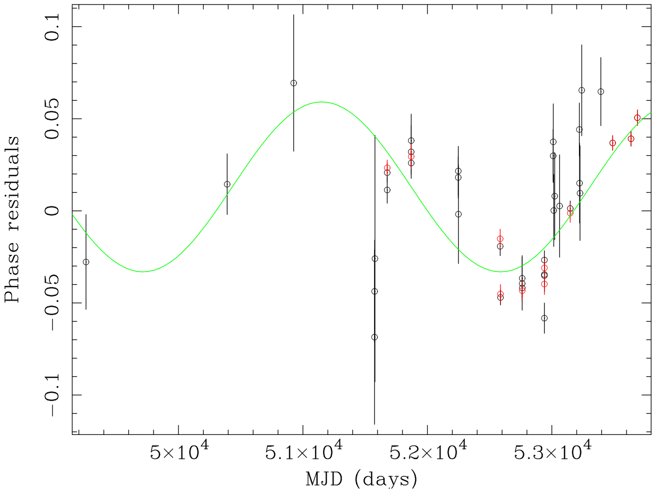

Fig. 7 Phase residuals for RX J0720.4–3125. The black data points are reproduced from Kaplan & van Kerkwijk (2005a) while red points are from the analysis of Haberl et al. (2006), which includes a re-analysis of published EPIC-pn results for a consistency check as well as three new data sets (the last three points).

Haberl et al. (2006) used a polar cap model similar to that applied by Schwope et al. (2005) to RBS 1223. Including free precession of the neutron star to explain the long-term spectral variations of RX J0720.4–3125 they can at least qualitatively reproduce the variations in the X-ray spectra, changes in the pulsed fraction, shape of the light curve and the phase-lag between soft and hard energy bands. Like for RBS 1223, where the intensity peaks in the pulse profile are not separated by 0.5 in spin phase, the spots on the surface of RX J0720.4–3125 are probably also not located exactly in antipodal positions. This can explain the observed evolution of the light curve and hardness ratio with precession phase.

4 Discussion

The new results from optical and X-ray observations of the Magnificent Seven, thermally emitting isolated neutron stars, strongly support the model of cooling neutron stars with ages around a million years. Large proper motions measured for the three brightest objects make accretion from the interstellar medium to re-heat the neutron star very inefficient. Absorption features in the X-ray spectra of most of the Magnificent Seven and first measurements of the spin period derivative from the two pulsars RX J0720.4–3125 and RBS 1223 consistently point to magnetic field strengths of the order of 10^{13} G to 10^{14} G. This places them at the long spin period and high magnetic field end of the radio pulsar distribution. However, the $\dot{P}$ measurements still indicate field strengths below those of the magnetars (Fig. 8). The discovery of a few radio pulsars with similar magnetic field strengths and long periods (Camilo et al. 2000; Morris et al. 2002; McLaughlin et al. 2003) shows that radio emission can still occur at inferred field strengths close to the "quantum critical field" $B_{cr} = m_e^2 c^3/e\hbar \simeq 4.4 \times 10^{13}$ G. Therefore it remains unclear if the M7 exhibit no radio emission at all or if we do not detect them because their radio beam is very narrow due to their large light cylinder radius and therefore does not cross the Earth.

In a $\sim 10^{13}$ G magnetic field cyclotron resonance lines at soft X-ray energies are expected to be caused by protons or highly ionized atoms of heavy elements. The ratios of line strengths in consecutive harmonic lines scales with $E_{cyc}/(mc^2)$ (Pavlov et al. 1980) and for the involved high particle masses no harmonic lines should be detectable. There is now more and more evidence for additional absorption lines in the X-ray spectra of the Magnificent Seven. An explanation for the additional (or even all) lines can be atomic bound-bound or bound-free transitions. In high B fields atomic orbitals are distorted into a cylindrical shape and the electron energy levels are similar to Landau states, with binding energies of atoms strongly increased. For hydrogen in a magnetic field of the order of 10^{13} G the strongest atomic transition is expected at energy $E/eV \approx 75(1+0.13\ln(B_{13}))+63B_{13}$, with $B_{13} = B/10^{13}$ G (Zavlin & Pavlov 2002). For the line energies found in the spectra of thermal isolated neutron stars this requires similar field strengths to those derived assuming cyclotron absorption. Atomic line transitions are expected to be less prominent at higher temperatures because of a higher ionization degree (Zavlin & Pavlov 2002). For a more detailed discussion of expected line features that can be produced in a hydrogen atmosphere see van Kerkwijk & Kaplan (2006). It is also not clear how important the contribution of heavier elements in the

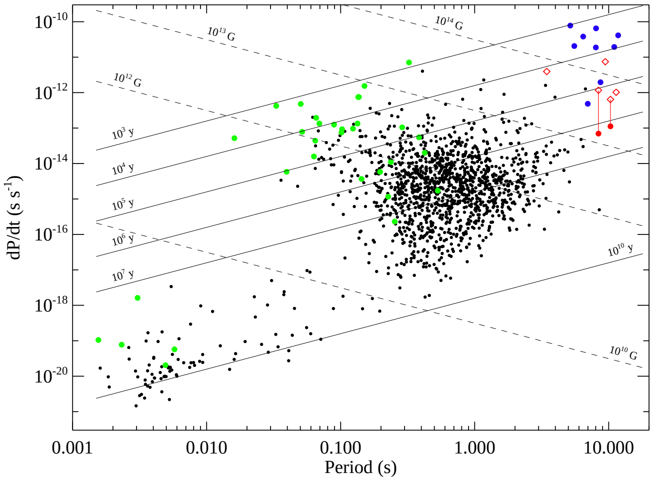

Fig. 8 $P - \dot{P}$ diagram for radio pulsars (black dots), magnetars (blue dots) and the Magnificent Seven. Red dots show the direct P and $\dot{P}$ measurements for RX J0720.4–3125 and RBS 1223, while the open diamonds mark the $\dot{P}$ values expected from the magnetic field estimates assuming proton resonance as origin of the absorption lines. For RX J0720.4–3125 and RBS 1223 both field estimates are connected with a vertical line. Marked in green are radio pulsars which are also detected at high energies (incomplete for the millisecond pulsars).

atmosphere is because of the strong gravitational stratification forces (Mori & Hailey 2006). Further, the remarkable harmonic-like energy spacing of multiple lines needs to be understood. Studying their pulse phase dependence which can probably best be done for RBS 1223 might shed light on this.

The modeling of pulse profiles in different X-ray energy bands is a powerful tool to unveil the surface temperature distribution of the neutron stars (Zane & Turolla 2006). First studies of RX J0720.4–3125 and RBS 1223 yielded constraints on the polar cap geometry. It is remarkable that for both stars asymmetric configurations of the hot polar caps were inferred. In both cases different temperatures and sizes of the hot spots are found with the smaller spot being the hotter one. Probably, also in both stars the spots are not located in exactly antipodal positions. This could point to magnetic field configurations of an off-centered dipole or the involvement of higher-order multi-pole components. Studies of the effects of a strong magnetic field on the temperature distribution in the neutron star crust show that configurations which include dipolar poloidal and toroidal components can indeed reproduce the observed temperature distributions (Geppert et al. 2004, 2006).

Acknowledgements The XMM-Newton project is an ESA Science Mission with instruments and contributions directly funded by ESA Member States and the USA (NASA). The XMM-Newton project is supported by the Bundesministerium für Wirtschaft und Technologie/Deutsches Zentrum für Luft- und Raumfahrt (BMWI/DLR, FKZ 50 OX 0001), the Max-Planck Society and the Heidenhain-Stiftung.

References

Agüeros, M. A., Anderson, S. F., Margon, B., et al. AJ, **131**, 1740 (2006)

Akgün, T., Link, B., & Wasserman, I. MNRAS, **365**, 653 (2006)

Braje, T. M. & Romani, R. W. ApJ, **580**, 1043 (2002)

Burwitz, V., Haberl, F., Neuhäuser, R., et al. A&A, **399**, 1109 (2003)

Burwitz, V., Zavlin, V. E., Neuhäuser, R., et al. A&A, **379**, L35 (2001)

Camilo, F., Kaspi, V. M., Lyne, A. G., et al. ApJ, **541**, 367 (2000)

Chieregato, M., Campana, S., Treves, A., et al. A&A, **444**, 69 (2005)

Cropper, M., Haberl, F., Zane, S., & Zavlin, V. E. MNRAS, **351**, 1099 (2004)

Cropper, M., Zane, S., Ramsay, G., Haberl, F., & Motch, C. A&A, **365**, L302 (2001)

de Vries, C. P., Vink, J., Méndez, M., & Verbunt, F. A&A, **415**, L31 (2004)

Gänsicke, B. T., Braje, T. M., & Romani, R. W. A&A, **386**, 1001 (2002)

Geppert, U., Küker, M., & Page, D. A&A, **426**, 267 (2004)

Geppert, U., Küker, M., & Page, D. A&A, in press, astro-ph/0512530 (2006)

Haberl, F. Advances in Space Research, **33**, 638 (2004)

Haberl, F. in 5 years of Science with XMM-Newton, MPE Report **288**, 39–44 (2005)

Haberl, F., Motch, C., Buckley, D. A. H., Zickgraf, F. J., & Pietsch, W. A&A, **326**, 662 (1997)

Haberl, F., Motch, C., Zavlin, V. E., et al. A&A, **424**, 635 (2004a)

Haberl, F., Schwope, A. D., Hambaryan, V., Hasinger, G., & Motch, C. A&A, **403**, L19 (2003)

Haberl, F., Turolla, R., de Vries, C. P., et al. A&A, **451**, L17 (2006)

Haberl, F. & Zavlin, V. E. A&A, **391**, 571 (2002)

Haberl, F., Zavlin, V. E., Trümper, J., & Burwitz, V. A&A, **419**, 1077 (2004b)

Hambaryan, V., Hasinger, G., Schwope, A. D., & Schulz, N. S. A&A, **381**, 98 (2002)

Ho, W. C. G. & Lai, D. ApJ, **607**, 420 (2004)

Johnston, S. MNRAS, **340**, L43 (2003)

Jones, D. I. & Andersson, N. MNRAS, **324**, 811 (2001)

Kaplan, D. L., Kulkarni, S. R., & van Kerkwijk, M. H. ApJ, **579**, L29 (2002a)

Kaplan, D. L., Kulkarni, S. R., & van Kerkwijk, M. H. ApJ, **588**, L33 (2003a)

Kaplan, D. L., Kulkarni, S. R., van Kerkwijk, M. H., & Marshall, H. L. ApJ, **570**, L79 (2002b)

Kaplan, D. L. & van Kerkwijk, M. H. ApJ, **628**, L45 (2005a)

Kaplan, D. L. & van Kerkwijk, M. H. ApJ, **635**, L65 (2005b)

Kaplan, D. L., van Kerkwijk, M. H., & Anderson, J. ApJ, **571**, 447 (2002c)

Kaplan, D. L., van Kerkwijk, M. H., Marshall, H. L., et al. ApJ, **590**, 1008 (2003b)

Ketsaris, N. A., Kuster, M., Postnov, K. A., et al. in Proc. Intl. Workshop: Hot Points in Astrophysics, JINR, Dubna, Russia, 192–205 (2000)

Komarova, V. in Isolated Neutron Stars: From the surface to the interior, these conference proceedings (2006)

Malofeev, V. M., Malov, O. I., & Teplykh, D. A. in Isolated Neutron Stars: From the surface to the interior, these conference proceedings (2006a)

Malofeev, V. M., Malov, O. I., Teplykh, D. A., et al. The Astronomer's Telegram, **798**, 1 (2006b)

McLaughlin, M. A., Stairs, I. H., Kaspi, V. M., et al. ApJ, **591**, L135 (2003)

Mori, K. & Hailey, C. J. ApJ, submitted, astro-ph/0301161v2

(2006)

Morris, D. J., Hobbs, G., Lyne, A. G., et al. MNRAS, **335**, 275 (2002)

Motch, C. in X-ray Astronomy, Stellar Endpoints, AGN, and the Diffuse X-ray Background, AIP Conference Proceedings, 244–253 (2001)

Motch, C., Haberl, F., Zickgraf, F. J., Hasinger, G., & Schwope, A. D. A&A, **351**, 177 (1999)

Motch, C., Mancini-Pires, A., Haberl, F., & Schwope, A. D. in Isolated Neutron Stars: From the surface to the interior, these conference proceedings (2006)

Motch, C., Sekiguchi, K., Haberl, F., et al. A&A, **429**, 257 (2005)

Motch, C., Zavlin, V. E., & Haberl, F. A&A, **408**, 323 (2003)

Paerels, F. ApJ, **476**, L47 (1997)

Paerels, F., Mori, K., Motch, C., et al. A&A, **365**, L298 (2001)

Page, D., Geppert, U., & Weber, F. Nuclear Physics B, in press, astro-ph/0508056 (2006)

Pavlov, G. G., Shibanov, I. A., & Iakovlev, D. G. Astrophysics and Space Science, **73**, 33 (1980)

Pavlov, G. G., Zavlin, V. E., & Sanwal, D. in Neutron Stars, Pulsars, and Supernova Remnants, Eds. W. Becker, H. Lesch and J. Trümper, MPE-Report **278**, 273–286 (2002)

Pavlov, G. G., Zavlin, V. E., Trümper, J., & Neuhäuser, R. ApJ, **472**, L33 (1996)

Pons, J. A., Walter, F. M., Lattimer, J. M., et al. ApJ, **564**, 981 (2002)

Posselt, B., Popov, S. B., & Haberl, F. in Isolated Neutron Stars: From the surface to the interior, these conference proceedings (2006)

Ransom, S. M., Gaensler, B. M., & Slane, P. O. ApJ, **570**, L75 (2002)

Rutledge, R. E., Fox, D. W., Bogosavljevic, M., & Mahabal, A. ApJ, **598**, 458 (2003)

Schwope, A. D., Hambaryan, V., Haberl, F., & Motch, C. A&A, **441**, 597 (2005)

Schwope, A. D., Hambaryan, V., Haberl, F., & Motch, C. in Isolated Neutron Stars: From the surface to the interior, these conference proceedings (2006)

Schwope, A. D., Hasinger, G., Schwarz, R., Haberl, F., & Schmidt, M. A&A, **341**, L51 (1999)

Treves, A., Turolla, R., Zane, S., & Colpi, M. PASP, **112**, 297 (2000)

Trümper, J. E., Burwitz, V., Haberl, F., & Zavlin, V. E. Nuclear Physics B Proceedings Supplements, **132**, 560 (2004)

Trümper, J., Kahabka, P., Oegelman, H., Pietsch, W., & Voges, W. ApJ, **300**, L63 (1986)

van Kerkwijk, M. H. & Kaplan, D. in Isolated Neutron Stars: From the surface to the interior, these conference proceedings (2006)

van Kerkwijk, M. H., Kaplan, D. L., Durant, M., Kulkarni, S. R., & Paerels, F. ApJ, **608**, 432 (2004)

van Kerkwijk, M. H. & Kulkarni, S. R. A&A, **380**, 221 (2001a)

van Kerkwijk, M. H. & Kulkarni, S. R. A&A, **378**, 986 (2001b)

Vink, J., de Vries, C. P., Méndez, M., & Verbunt, F. ApJ, **609**, L75 (2004)

Walter, F. M. ApJ, **549**, 433 (2001)

Walter, F. M. & Lattimer, J. M. ApJ, **576**, L145 (2002)

Walter, F. M. & Matthews, L. D. Nature, **389**, 358 (1997)

Walter, F. M., Wolk, S. J., & Neuhäuser, R. Nature, **379**, 233 (1996)

Zampieri, L., Campana, S., Turolla, R., et al. A&A, **378**, L5 (2001)

Zane, S., Cropper, M., Turolla, R., et al. ApJ, **627**, 397 (2005)

Zane, S., Haberl, F., Cropper, M., et al. MNRAS, **334**, 345 (2002)

Zane, S. & Turolla, R. MNRAS, **366**, 727 (2006)

Zane, S., Turolla, R., Stella, L., & Treves, A. ApJ, **560**, 384 (2001)

Zavlin, V. E. & Pavlov, G. G. in Neutron Stars, Pulsars, and Supernova Remnants, Eds. W. Becker, H. Lesch and J. Trümper, MPE-Report **278**, 263–272 (2002)